Supplementary Information

Modular Protein-DNA Hybrid Nanostructures as a Drug Delivery Platform

Yiseul Ryu[a], Cheol Am Hong[b], Yunjin Song[a], Jonghwi Beak[a], Bo Am Seo[c], Joong-jae Lee*[a], and Hak-Sung Kim*[b]

[a]Department of Biochemistry, Kangwon National University, Chuncheon 24341, South Korea, E-mail: leejj@kangwon.ac.kr. [b]Department of Biological Sciences, Korea Advanced Institute of Science and Technology (KAIST), Daejeon 34141, South Korea, E-mail: hskim76@kaist.ac.kr. [c]Biomedical Science & Engineering Interdisciplinary Program, Korea Advanced Institute of Science and Technology (KAIST), Daejeon 34141, South Korea

I. Experimental Procedures

Preparation of zinc-finger domain (ZnF)-fused proteins

The genes of ZnF-fused proteins were cloned into a pET-21a (+) expression vector (Novagen, USA) using *NdeI* and *XhoI* restriction sites. The resulting recombinant vectors were transformed into BL21(DE3) host cells (Novagen, USA). A single colony expressing a designed ZnF-fused protein was grown overnight in Luria-Bertani (LB, Ambrothia, Korea) medium containing 100 μg/ml ampicillin (Amp; Duchefa Biochemie, Nederland) under a shaking incubator at 37°C. The resulting cells were diluted 100-fold into a fresh LB/Amp medium and further cultured. When an optical density at 600 nm (OD_{600}) reached 0.5, isopropyl β-D-1-thiogalactopyranoside (IPTG) and $ZnSO_4$ at final concentrations of 0.1 mM and 0.2 mM, respectively, were added and further incubated for 2 days at 18°C. The purification of ZnF-fused proteins was performed by a previously reported method[1] with slight modifications. Briefly, the cells were harvested by centrifugation (Hitachi, Japan) at 6,000 rpm and the pellet was resuspended in a lysis buffer (20 mM Tris, 500 mM NaCl, 10 mM Imidazole, 0.2 mM $ZnSO_4$, 10 mM Dithiothreitol (DTT), and pH 8.0) with an EDTA-free protease inhibitor (Roche, Switzerland). After disrupting by a sonicator (Sonics, USA), the cell debris and insoluble fraction were removed by centrifugation at 13,000 rpm for 1 h at 4°C. The resulting supernatant was filtered using a 0.22 μm syringe filter (Millipore, USA) and the eluted solution was loaded into a nickel-charged affinity resin (Qiagen, USA). After washing three times with a washing buffer (20 mM Tris, 1000 mM NaCl, 20 mM Imidazole, 0.2 mM $ZnSO_4$, 10 mM DTT, and pH 8.0), the resin-bound ZnF-fused proteins were eluted using an elution buffer (20 mM Tris, 300 mM NaCl, 250 mM Imidazole, 0.2 mM $ZnSO_4$, 10 mM DTT, and pH 8.0). The purified ZnF-fused proteins were stored at 4°C prior to use, followed by identification of the desired products via SDS-PAGE analysis.

Construction of functional Y-shaped DNA nanostructures (FYDN)

All single-stranded DNAs (ssDNAs; Integrated DNA Technologies, USA) used in the preparation of FYDNs were computationally designed by using NUPACK web server (http://www.nupack.org), and are presented in Figure S1. For effective self-assembly, we conducted a slow cooling method. Briefly, equal molar amounts of three different individual ssDNAs were mixed in 1x phosphate-buffered saline (PBS) buffer (pH 7.4), and after melted at 95°C for 2 min, temperature was gradually decreased from 95°C until reaching 10°C at a

rate of -1.0°C per 1 min using a thermal cycler (Thermo Fisher, USA). The resulting products, Y-shaped DNA (Y-DNA), were used without the need for additional purification steps. To prepare FYDNs, 100 nM of a Y-DNA and 300 nM of ZnF-fused proteins were incubated in a ZnF-binding buffer (20 mM Tris, 250 mM NaCl, 0.2 mM $ZnSO_4$, 1 mM $MgCl_2$, 2 mM beta-mercaptoethanol, 0.1 mg/ml bovine serum albumin (BSA), 0.01% CA-630, 1% glycerol, and pH 8.0) for 30 min at room temperature. Unbound ZnF-fused proteins were removed by centrifugal filtration (100 kDa MWCO, Millipore, USA) three times with ZnF-binding buffer at 4,000 rpm for 5 min at 25°C. The final concentration of FYDNs was estimated by using Qubit 4 Fluorometer (Thermo Fisher, USA) with Qubit 4™ dsDNA BR assay kit. All final products were stored at 4°C for a maximum of 1 month prior to use.

Transmission electron microscopy (TEM)

A well-defined Y-DNA was incubated with albumin-binding domain (ABD)-fused ZnF proteins in a ZnF-binding buffer (as described above) for 30 min at room temperature. The resulting FYDNs were incubated with 20-fold molar excess of human serum albumin (HSA)-passivated gold nanoparticles, and then purified and visualized as reported in a previous study.[2] Briefly, centrifugation for removal of unbound HSA-passivated gold nanoparticles was performed and the final products were dropped onto a meshed carbon coated grid (Electron Microscopy Sciences, USA) and then air-dried for 1 h. TEM images were obtained by using a 200 kV field-emission source transmission electron microscope (JEOL, Japan).

Nuclease resistance

Y-DNA (100 nM) and FYDNs (100 nM) were incubated with 100 units/ml of exonuclease III (New England Biolabs, USA) for 1 h or 6 h at room temperature, and then 10 μM of DNA-intercalating YOYO-1 dyes (Invitrogen, USA) were further treated to the mixture for 5 min. The fluorescence spectrum of the resulting products was estimated using a microplate reader (Tecan, Switzerland). The levels of DNA degradation were calculated using the formula: $(F_0 - F)/F_0 \times 100$. The F_0 and F indicate the fluorescence intensity of YOYO-1 dyes at 515 nm in the absence and presence of exonuclease, respectively.

Confocal fluorescence microscopy

MDA-MB-468, HCC827, RL95-2, and MCF7 cells were cultured in RPMI 1640 media (Hyclone, USA) at 37°C in an incubator (Sanyo, Japan) with 5% CO_2, and A431 cells were

grown in DMEM media (Hyclone, USA). All culture media were supplemented with 10% heat-inactivated fetal bovine serum (FBS; Gibco, USA). The cells were seeded in an 8-well glass slide (SPL Life Sciences, Korea) at a density of 0.5×10^5 cells/well for 24 h incubation. EGFR-targeting FYDNs (100 nM), non-targeting FYDNs (100 nM), and EGFR-targeting FYDN-Dox (1 μM) were incubated with the cells for 3 h or 24 h. After washing three times with Dulbecco's Phosphate-Buffered Saline (DPBS) (Thermo Fisher, USA), the cells were fixed using 4% paraformaldehyde at 4°C for 1 h, and then stained with DAPI (Vector laboratories, USA) or Hoechst 33342 (ThermoFisher, USA) solution for nucleus detection. Fluorescence images of the resulting cells were obtained using a confocal microscopy (Carl Zeiss, Germany) with 400x magnification.

Fluorescence resonance energy transfer (FRET) analysis

The solution of EGFP-NRE and mCherry-Zif268 or EGFP-NRE, mOrange-QNK, and mCherry-Zif268 (300 nM) were co-incubated with Y-DNA (100 nM) in a ZnF-binding buffer (as described above) for 30 min at room temperature. After incubation, the fluorescence intensities of these fluorescent protein mix solutions with Y-DNA or without Y-DNA (as a negative control) were measured by microplate reader for fluorescence (Biotek, USA). To observe the FRET signal, donor emission (515 nm) and acceptor emission (607 nm) was measured at 488 nm excitation wavelength. In three color FRET analysis, in order to exclude the possibility of mOrange excitation itself, acceptor emission (607 nm) was measured at 390 nm excitation wavelength.

Enzyme-linked immunosorbent assay (ELISA)

Various antigens (10 μg/ml) were coated onto a 96-well Maxisorp plate (SPL Life Sciences, Korea) at 4°C for overnight. Bovine serum albumin (BSA) was used as a control. The resulting antigen-coated well plates were washed three times with a washing buffer (PBS supplemented with 0.1% Tween 20; PBST), and blocked with a blocking buffer (PBST supplemented with 20 mg/ml BSA and 0.2 mM $ZnSO_4$) for 1 h at room temperature. After washing with 1x PBS, biotinylated EGFR-targeting FYDNs (10 nM) dissolved in a blocking buffer was added into each well and incubated for 1 h at room temperature. After washing with a blocking buffer, the ELISA signals were developed using a subsequent incubation of a 1:1000 dilution of HRP-conjugated streptavidin (Bio-Rad, USA) and 3,3',5,5'-tetramethylbenzidine (TMB; Sigma Aldrich, USA). After addition of 1 N H_2SO_4 solution, the

developed signals were measured at 450 nm using a microplate reader (Tecan, Switzerland). Bi-specificity of the dual-targeting FYDNs (EGFRxIL-6 or EGFRxHER2) were also confirmed using a bridging ELISA method. Briefly, following antigen coating and blocking, dual-targeting FYDNs (10 nM) were applied to each antigen-coated well. Secondary antigens (10 μg/ml), biotinylated human IL-6 or human HER2-Fc (Sino Biological, Inc, China), were incubated for 1 h. After washing three times, HRP-conjugated streptavidin or HRP-conjugated anti-human IgG (Fc specific) antibody (Bio-Rad, USA) was added for signal development.

Doxorubicin intercalation assay

Varying concentration of Y-DNA nanostructures was incubated with 1 μM of Doxorubicin (Sigma, USA) at room temperature for 1 h, followed by washing 3 times via centrifuge as described above. The fluorescence spectrum of Dox-intercalating Y-DNAs was obtained using a 96-well black plate (SPL, Korea) and a microplate reader (Tecan, Switzerland) for determining a Dox-intercalating condition as shown in Figure S9a. Y-DNA nanostructure was expected to have 10 sites of theoretically predicted doxorubicin intercalation sites (GC/CG). Therefore, we estimated the equivalent Dox concentration of FYDNs based on the rationale as described in elsewhere.[3,4]

***In vitro* cell viability assay**

To assess the cell viability of EGFR-targeting FYDN-Dox, A431 cells ($EGFR^{high}$) and MCF7 cells ($EGFR^{low}$) were seeded onto a 96-well flat bottom culture plate (SPL Life Sciences, Korea) at a density of 3×10^3 cells/well. After 24 h incubation, the cells were washed three times with 1x DPBS, and incubated with EGFR-targeting FYDN-Dox or Dox alone for 72 h. For the cytotoxicity of EGFR-targeting FYDN and PTEN, A431 cells and HCC827 cells (Erlotinib sensitive) and RL95-2 cells (Erlotinib resistant) were seeded onto a 96-well flat bottom cell culture plate (3×10^3 cells/well) and grown for 24 h. The cells were treated with EGFR-targeting FYDNs (Y-DNA/anti-EGFR specific repebody; rbEGFR/PTEN) and a mixture of EGFR-targeting FYDNs (Y-DNA/rbEGFR/PTEN) and 1 μM of Erlotinib (Selleckchem, USA) at varying concentrations of FYDNs for 72 h. The half-maximal inhibitory concentration (IC50) was measured by Sigmaplot software (Systat Software, USA). All cell viability assay was performed in triplicate and determined according to the cell counting kit-8 protocol (CCK-8; Dojindo Molecular Technologies, Japan).

Western blot analysis

RL95-2 cells were seeded onto a 6-well plate (SPL Life Sciences, Korea) at a density of 3 × 10^5 cells/well in 5 ml of the medium for 24 h incubation. The cells were incubated with EGFR-targeting FYDNs (Y-DNA/rbEGFR/PTEN, 500 nM). After 72 h incubation, the cells were washed three times with a Tris-buffered saline (TBS), and then lysed with 0.5 ml of a RIPA lysis buffer (Millipore, USA) containing a phosphatase inhibitor (Roche, Switzerland). The resulting cell lysates were subjected to centrifugation at 13,000 rpm for 10 min at 4°C. The supernatant was analyzed using a 4-20% SDS-PAGE gradient gel (Bio-Rad, USA) after heating at 95°C for 5 min. The proteins were transferred to a polyvinylidene difluoride (PVDF) membrane (Bio-Rad, USA) at 100 V for 1 h, and the membrane was blocked with a blocking solution (TBS containing 1% BSA; TBST) for 1 h. The primary antibody, Phospho-Akt (Ser473) antibody (Dilution 1:5000; Cell Signaling Technology, USA) or beta-actin antibody (Dilution 1:10000; Sigma, USA), was dissolved in a blocking buffer supplemented with 0.02 % sodium azide, and incubated with the blocked membranes at 4°C for overnight, followed by 1 h incubation with anti-rabbit IgG, HRP-conjugated antibody (Dilution 1:10000; Pierce, USA). The signals were developed using an enhanced chemiluminescence (ECL) solution (Millipore, USA), and detected through an imaging system (Bio-Rad, USA). The band intensity was estimated using Image J program (NIH, USA).

II. Supplementary Results

>a-strand (QNK-NRE)
ATATTTCTGCCTCTGCTGGATCCGCATGACATTCGCCGTAAGCGCAAGGGTTCAatat

>b-strand (NRE-Zif268)
ATATTGAACCCTTGCGCTTACGGCGAATGACCGAATCAGCCTGCTGCGTGGGCGatat

>c-strand(Zif268-QNK)
ATATCGCCCACGCAGCAGGCTGATTCGGTTCATGCGGATCCAGCAGAGGCAGAAatat

- AAGGGTTCA: **NRE** binding site
- GCGTGGGCG: **Zif268** binding site
- GAGGCAGAA: **QNK** binding site

Figure S1. Complete DNA sequences of each strand used for the self-assembly of a Y-DNA nanostructure bearing the three different zinc-finger binding domains. The NRE, Zif268, and QNK binding sites on a Y-DNA were colored in purple, blue, and yellow, respectively. All DNA sequences were presented in the 5' to 3' direction.

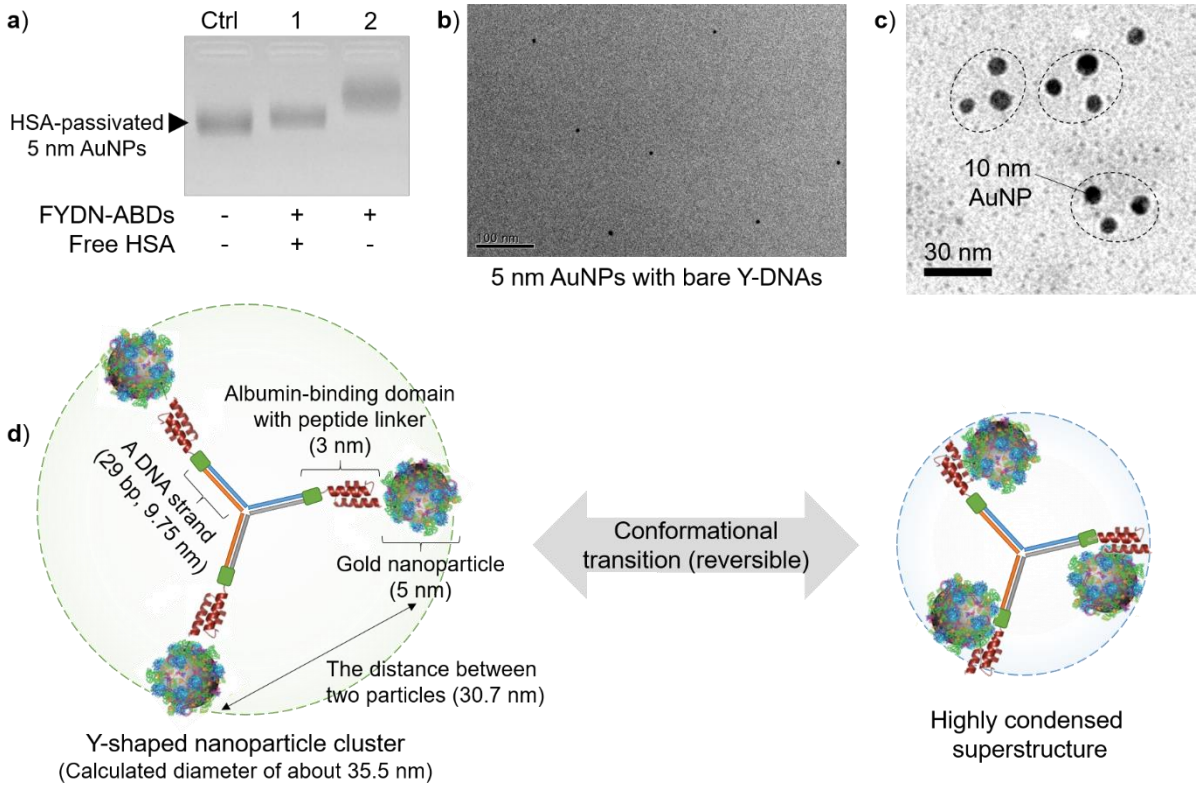

Figure S2. a) Agarose gel shift assay to verify the clustering of AuNPs based on functional Y-DNA nanostructures (FYDNs). FYDN was decorated with three different types of albumin binding domain (ABD)-fused zinc fingers (ZnFs). Free human serum albumin (HSA) was co-incubated with FYDN-ABDs (Sample 1), and used to block albumin binding sites of ABDs. Agarose gel shift assay showed that the formation of AuNP clusters is depended on the biological activity of ABDs loaded on FYDNs. **b**) TEM images of a mixture of human serum albumin-passivated 5 nm gold nanoparticles (AuNPs) and bare Y-DNA (without albumin-binding domains) at a magnification of 40,000x (Scale bar = 100 nm). **c**) Representative TEM image of Y-shaped AuNP clusters (Y-shaped NPCs) with 10 nm AuNPs. Raw TEM images were presented in Figure S3. The Y-shaped NPCs showed an enlarged superstructure than 5 nm AuNP-based one with a diameter of 40 nm. **d**) A schematic drawing of Y-shaped NPCs. The length of each arm of an extended Y-DNA is approximately 9.8 nm, and the distance between AuNPs is about 30.7 nm, resulting in the theoretical size of a fully stretched Y-shaped NPC (left) with the size of 35.5 nm. The Y-shaped NPCs could undergo a transition between the stretched form and a compacted conformation (right), due to the structural flexibility of biomolecules.

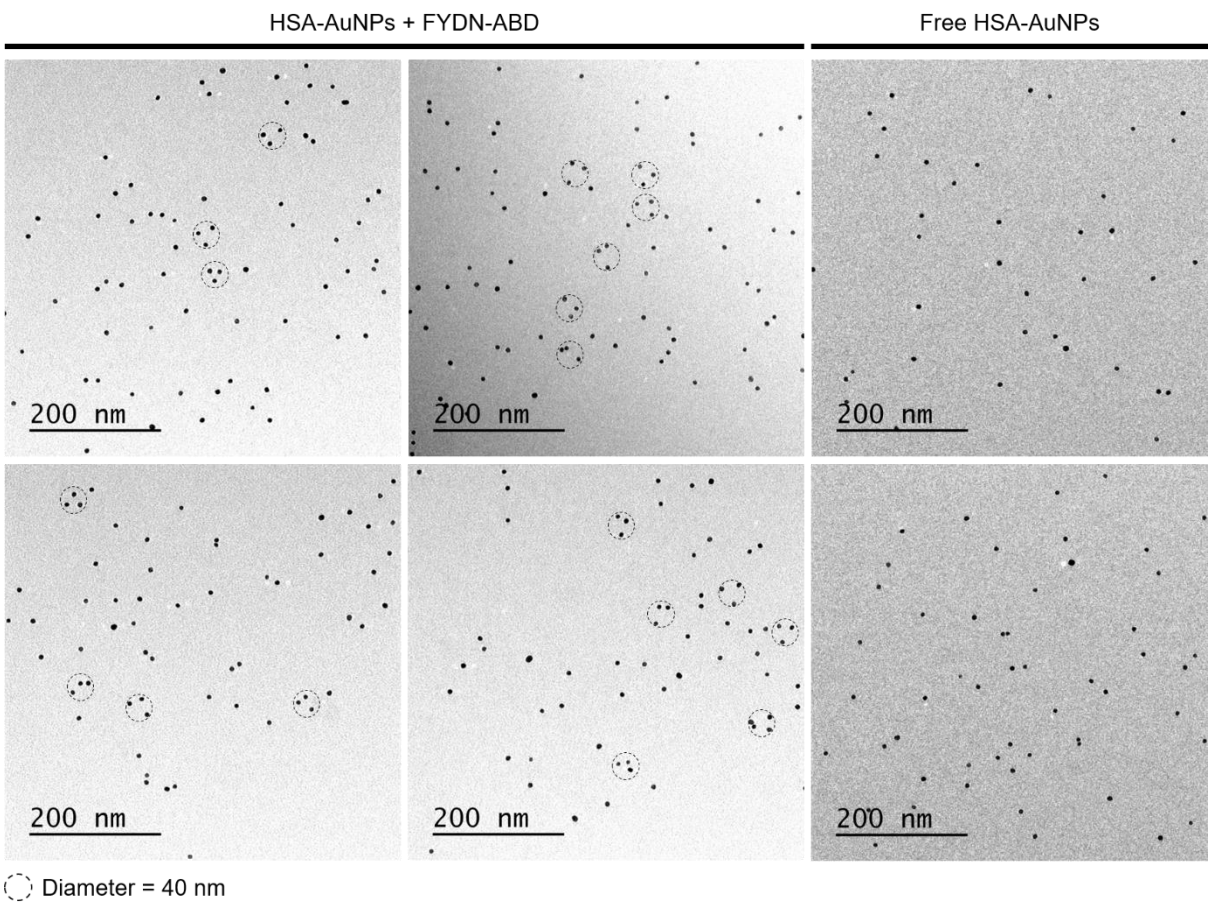

Figure S3. Visualization of gold nanoparticle (AuNP) clusters using transmission electron microscopy (TEM). We analyzed the formation of Y-DNA nanoclusters in the presence or absence of albumin binding domain (ABD)-functionalized Y-DNA nanostructures (FYDNs). Open circles, dashed line correspond to the constructed Y-DNA nanoclusters which defined as three AuNPs within a diameter of about 40 nm.

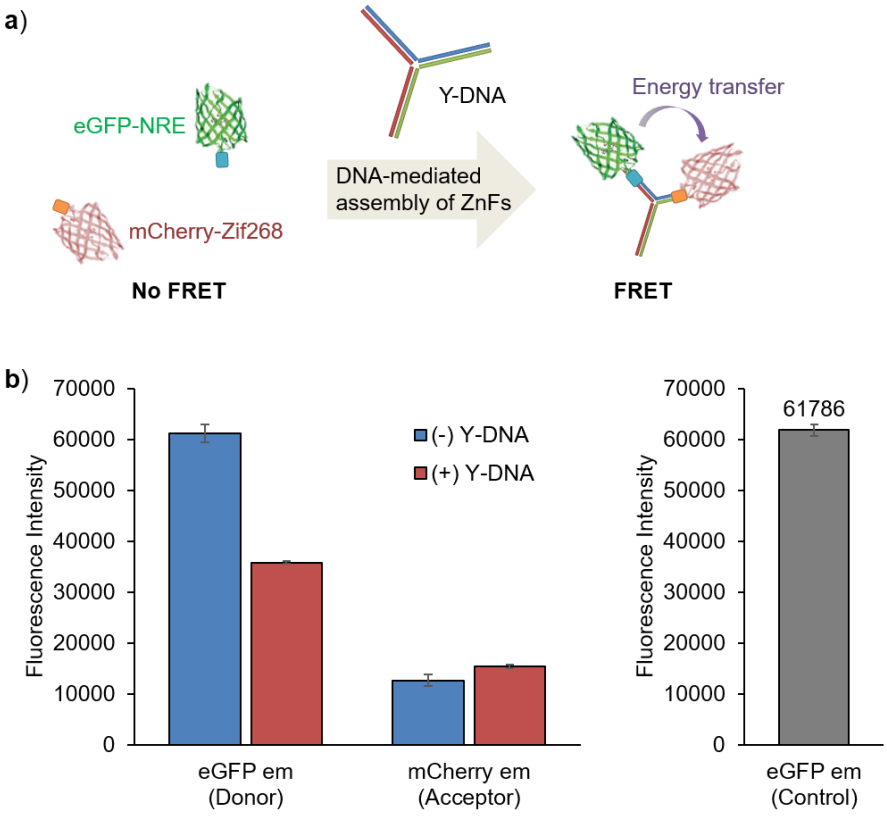

	eGFP emission	mCherry emission	FRET efficiency[1]	Distance (nm)[2]
(-) Y-DNA	61140	12669	-	-
(+) Y-DNA	35819	15393	0.42	5.58

[1]FRET efficiency (E) was calculated by the following equation: $E = 1 - (I_{DA} / I_D)$ where I_{DA} and I_D are the total eGFP (Donor) fluorescence intensities in presence and absence of mCherry (Acceptor), respectively. [2]DIstance between eGFP and mCherry was determined using the equation: $E(r) = 1 / [1 + (r / R^0)^6]$, where r = distance between eGFP and mCherry, and R^0 = Forster Radius = 5.288 nm.

Figure S4. Fluorescence resonance energy transfer (FRET) assay with two types of fluorescent protein (FP)-fused ZnFs for determining a distance between ZnF-fused proteins on a Y-DNA. **a)** A schematic design of FRET assay. Energy transfer from eGFP to mCherry occurs only in a Y-DNA-dependent manner due to the proximity of two proteins and spectral overlap of donor (eGFP) emission and acceptor (mCherry) absorption. **b)** Fluorescence intensities of two types of ZnF-fused FPs with or without Y-DNA. Compared to the fluorescent signals without Y-DNA (blue bar graph), a FRET phenomenon was clearly observed with Y-DNA as eGFP emission was reduced and mCherry emission was increased (red bar graph). Control indicates emission of eGFP alone. The data indicate the mean ± s.d. in triplicate experiments. The table below shows the measured fluorescence intensities, calculated FRET efficiency and estimated distance between eGFP and mCherry.

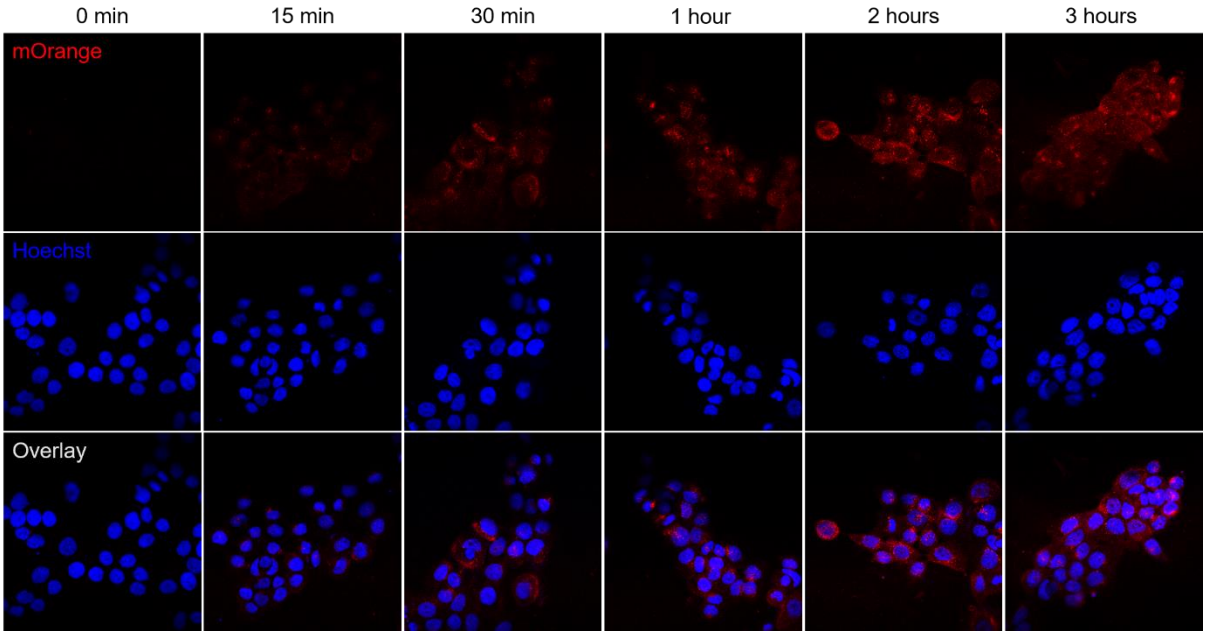

Figure S5. EGFR-medicated endocytosis of functional Y-DNA nanostructures (FYDNs) in a time-dependent manner. EGFR-targeting FYDNs (170 nM) with QNK-mOrange were incubated with EGFR-overexpressing A431 cells for the indicated times. Nuclei were counterstained with Hoechst 33342 dye. Confocal images exhibited that FYDN can be efficiently internalized into the cytoplasm within 1 hour.

a)

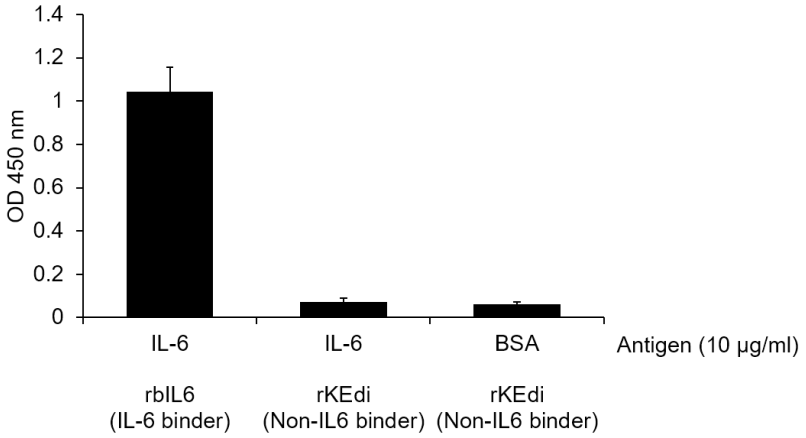

b) >rKEdi

```
ETITVSTPIKQIFPDDAFAETIKANLKKKSVTDAVTQNELNSIDQIKANNSDIKSVQGID
YLPNVRELALGGNKLHDISALKELTNLTDLTLEPNQLQSLPNGVFDKLTNLKELQLWANQ
LQSLPDGVFDKLTNLTYLNLAHNQLQDLPKGVFDKLTNLTELDLSYNQLQQLPKGVFDKL
TQLKDLELYQNQLKSVPDGVFDRLTSLQHIWLHDNPWDCTCPGIRYLSEWINKHSGVVRN
SAGSKAPDSAKCSGSGKPVRSIICPT
```

Figure S6. a) ELISA analysis of the binding property of repebodies for human interleukin-6 (IL-6). The IL-6 and BSA were coated at a concentration of 10 μg/ml. The resulting antigen-coated plates were incubated with various repebodies (100 μg/ml), and the binding signals were developed as described elsewhere.[1] BSA was used as a negative control. The data indicate the mean ± s.d. in triplicate experiments. **b**) Complete amino acid sequence of repebody-KEdi.

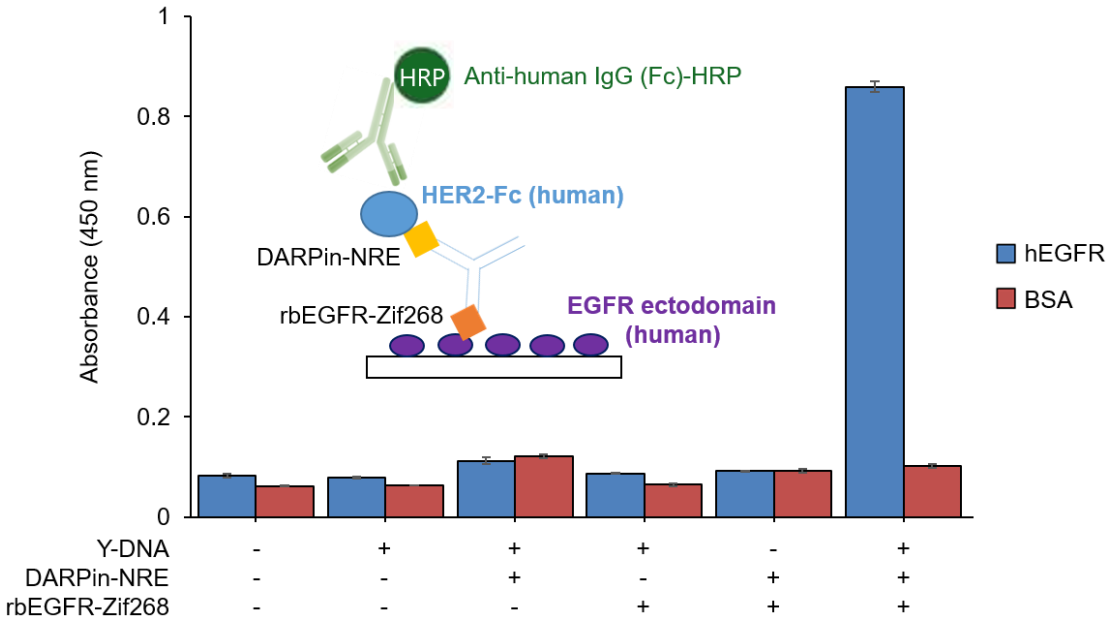

Figure S7. Modulation of the functionality of dual-targeting functional Y-DNA nanostructures (FYDNs). NRE-Zinc finger was genetically fused to HER2-specific DARpin-G3.[5] Dual-targeting FYDNs were simultaneously functionalized with DARPin-NRE and rbEGFR-Zif268, and incubated with each antigen-coated well on a 96-well plate. The concentration of coated antigens was 10 μg/ml. The data indicate the mean ± s.d. in triplicate experiments.

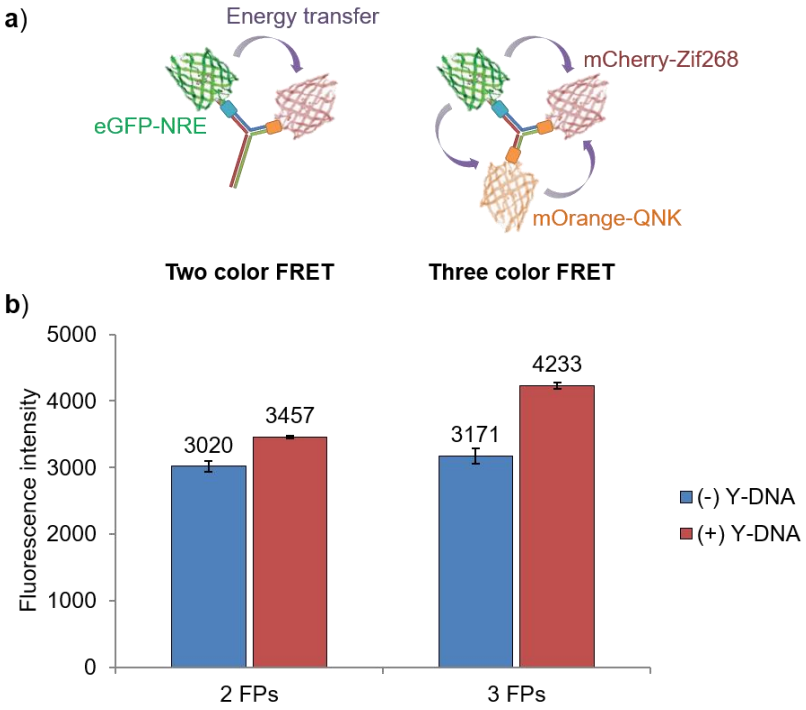

Figure S8. FRET assays using Y-DNAs with either two or three different types of fluorescent protein-fused ZnFs to show a controlled assembly of different ZnF proteins on a Y-DNA. **a**) A schematic design of assays. In three color FRET, an additional energy transfer occurs from eGFP to mOrange, and sequentially to mCherry. In this system, mCherry can receive more excitation energy from additional donor (mOrange) than regular two color FRET, resulting in an increase in FRET signals. **b**) Measurement of fluorescence intensities of the final acceptor (mCherry) in the two or three color FRET systems. Initial donor (eGFP) was excited at 390 nm of wavelength to exclude interference of the second donor (mOrange). The solutions containing two or three proteins only (blue bar graph) showed similar levels of mCherry emission. On the other hand, co-incubation with Y-DNA led to an enhanced mCherry signal in both systems. Interestingly, a significantly increased intensity was observed in three color FRET system (red bar graph), indicating that three different ZnFs were well-decorated on single Y-DNA molecules in a predesigned manner. The data indicate the mean ± s.d. in triplicate experiments.

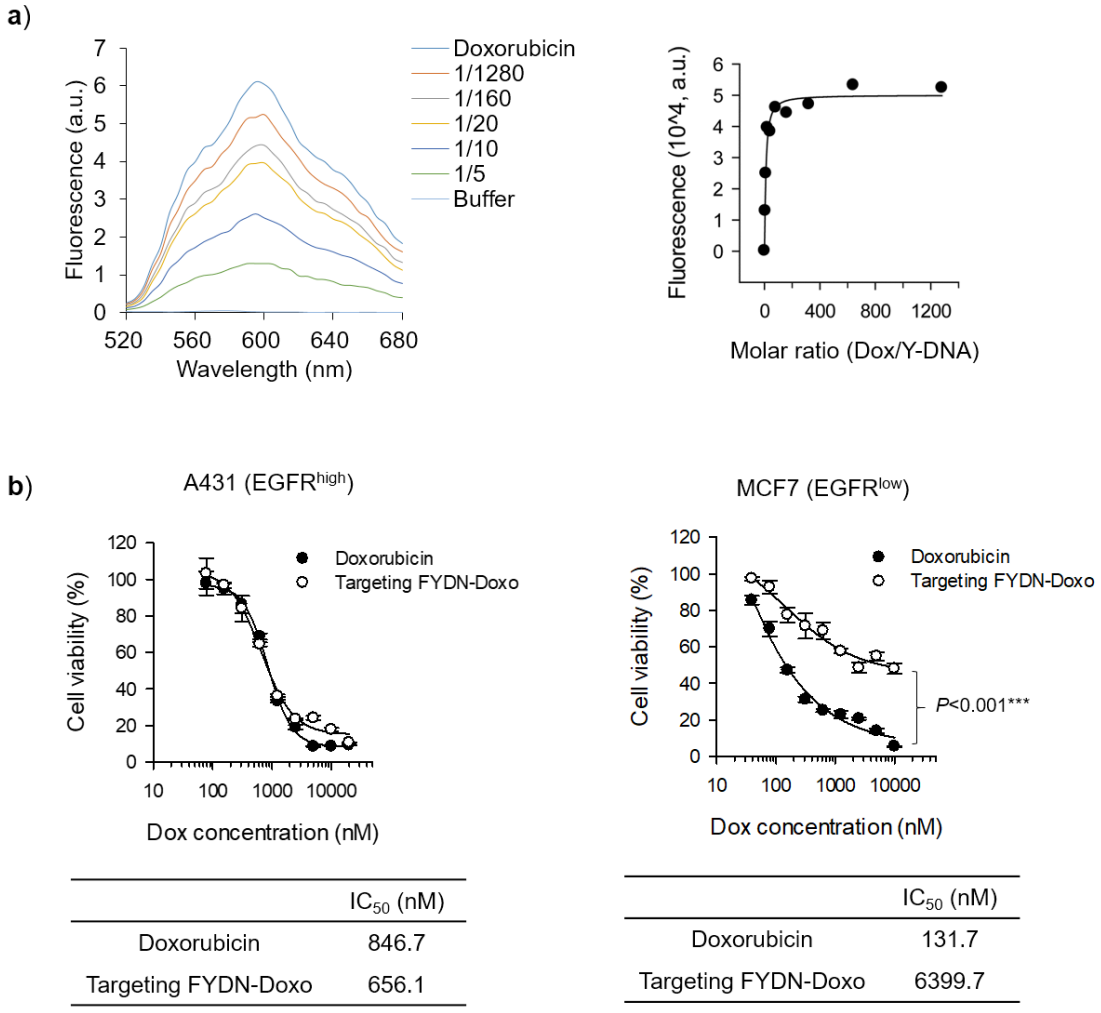

	IC_{50} (nM)
Doxorubicin	846.7
Targeting FYDN-Doxo	656.1

	IC_{50} (nM)
Doxorubicin	131.7
Targeting FYDN-Doxo	6399.7

Figure S9. a) The fluorescence spectra of Dox solution mixed with increasing molar ratios of Y-DNA (from top to bottom: Y-DNA/Dox molar ratio) (Left panel). The fluorescence intensity of Dox solution with increasing molar ratios of Dox/functional Y-DNA nanostructure (FYDN) at 595 nm (Right panel). The quenched Dox fluorescence was almost recovered at the Dox/Y-DNA molar ratio of 320:1. Based on the results, Dox-intercalating Y-DNAs were constructed at the Dox/Y-DNA molar ratio of 500:1. **b**) Dose-dependent viability of A431 cells expressing high level of EGFR($EGFR^{high}$) and MCF7 cells with low level of EGFR($EGFR^{low}$) after treated with Dox alone (black circles) and EGFR-targeting FYDNs (white circles). Binding specificity of EGFR-targeting FYDNs was validated using mOrange-decorated constructs by a confocal microscope (**Figure S10a**). The half maximal inhibitory concentration (IC_{50}) of EGFR-targeting FYDN-Dox and Dox alone were 656 nM and 847 nM for A431 cells, and 6400 nM and 132 nM for MCF7 cells, respectively. The data indicate the mean ± s.d. in triplicate experiments. ***$P < 0.001$ compared with Dox.

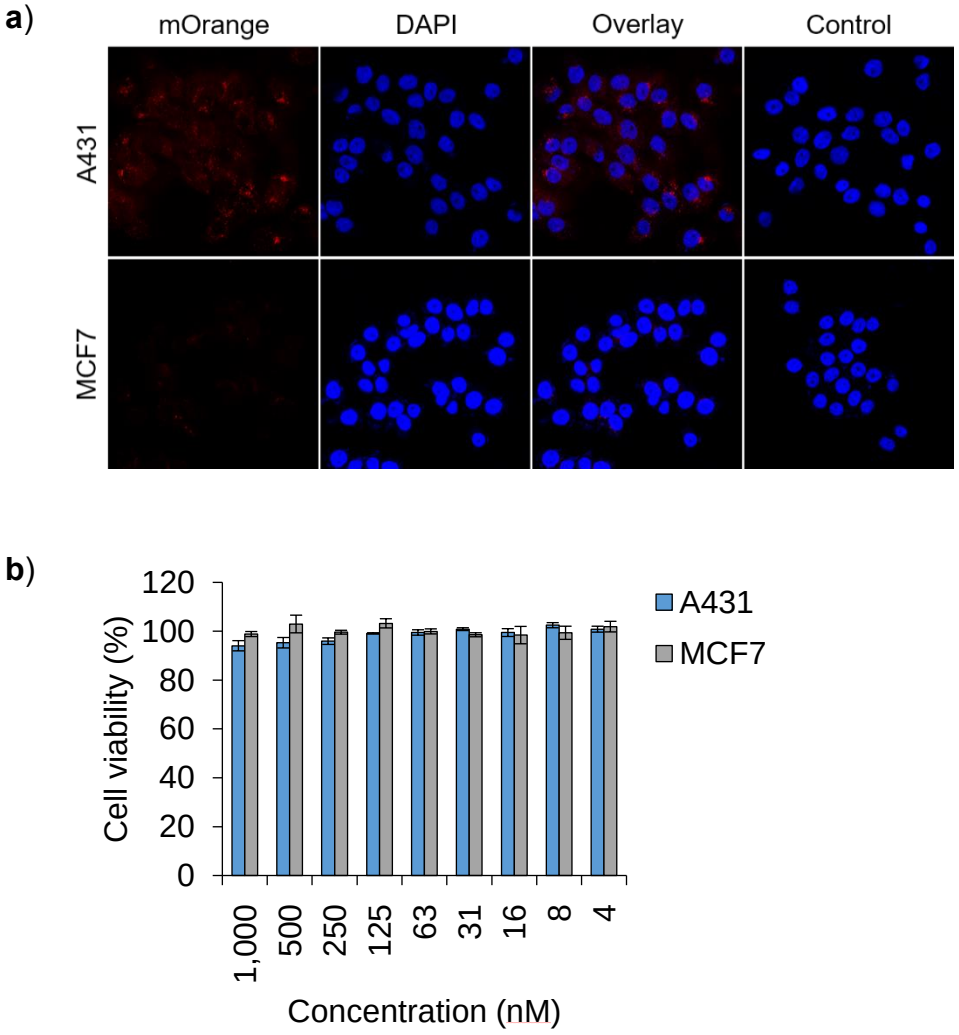

Figure S10. a) Binding ability of EGFR-targeting functional Y-DNA nanostructures (FYDNs) to EGFR at the cell surface. EGFR-targeting FYDNs (100 nM) were incubated with A431 ($EGFR^{high}$) and MCF7 cells ($EGFR^{low}$) for 3 h. Red color indicates mOrange bound to FYDNs. Cells with no treatment of FYDNs were used as control. **b**) Cytotoxicity of EGFR-targeting FYDNs on the cells after 72 h incubation at varying concentrations. The cell viability was measured on the basis of the untreated cells (set as 100%). The data indicate the mean ± s.d. in triplicate experiments.

>PTEN-QNK
MTAIIKEIVSRNKRRYQEDGFDLDLTYIYPNIIAMGFPAERLEGVYR
NNIDDVVRFLDSKHKNHYKIYNLCAERHYDTAKFNCRVAQYPFEDHN
PPQLELIKPFCEDLDQWLSEDDNHVAAIHCKAGKGRTGVMICAYLLH
RGKFLKAQEALDFYGEVRTRDKKGVTIPSQRRYVYYYSYLLKNHLDY
RPVALLFHKMMFETIPMFSGGTCNPQFVVCQLKVKIYSSNSGPTRRE
DKFMYFEFPQPLPVCGDIKVEFFHKQNKMLKKDKMFHFWVNTFFIPG
PEETSEKVENGSLCDQEIDSICSIERADNDKEYLVLTLTKNDLDKAN
KDKANRYFSPNFKVKLYFTKTVEEPSNPEASSSTSVTPDVSDNEPDH
YRYSDTTDSDPENEPFDEDQHTQITKVGSAGSAAGSGEKPYKCPGCG
KSFSQSSNLQKHQRTHTGEKPYKCPGCGKSFSQSSNLQKHQRTHTGE
KPYKCPGCGKSFSRSDHLSRHQRTHQNKLEHHHHHH

PTEN (Red)
QNK-ZnF domain (Blue)

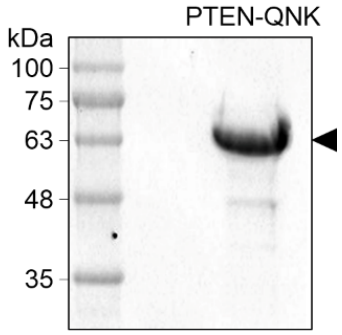

Figure S11. Complete amino acid sequence of ZnF-fused PTEN protein (PTEN-QNK) and SDS-PAGE analysis of purified PTEN-QNK. Amino acid sequences of PTEN and QNK zinc finger were colored in blue and red, respectively.

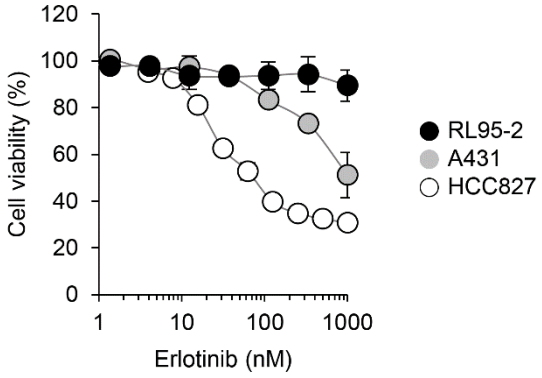

Figure S12. Viability of various cell types for identifying the resistance to Erlotinib. No significant reduction in the cell viability in RL 95-2 cells (Erlotinib resistant) treated with high-dose Erlotinib (up to 1000 nM) was observed compared to that of A431 and HCC827 cells (Erlotinb sensitive). The data indicate the mean ± s.d. in triplicate experiments.

III. References

[1] J. Lee, J. A. Kang, Y. Ryu, S. S. Han, Y. R. Nam, J. K. Rho, D. S. Choi, S. W. Kang, D. E. Lee, H. S. Kim, *Biomaterials* 2017, **120**, 22-31.

[2] Y. Ryu, Z. Jin, J. Lee, S. Noh, T. H. Shin, S. M. Jo, J. Choi, H. Park, J. Cheon, H. S. Kim, *Angew. Chem. Int. Ed.* 2015, **54**, 923-926.

[3] G. Zhu, J. Zheng, E. Song, M. Donovan, K. Zhang, C. Liu, W. Tan, *Proc. Natl. Acad. Sci. U.S.A.* 2013, **110**, 7998-8003.

[4] C. Pérez-Arnaiz, N. Busto, J. M. Leal, B. García, *J. Phys. Chem. B* 2014, **118**, 1288–1295.

[5] C. Zahnd, E. Wyler, J. M. Schwenk, D. Steiner, M. C. Lawrence, N. M. McKern, F. Pecorari, C. W. Ward, T. O. Joos, A. Plückthun, *J. Mol. Biol.* 2007, **369**, 1015–1028.

IV. Author Contributions

Y. Ryu and J. Lee conceived the idea, designed and constructed research materials, and performed the experiments. C. A. Hong constructed research materials, and performed the experiments. Y. J. Song, J. Beak, and B. A. Seo supported the experiments. Y. Ryu, C. A. Hong, J. Lee, and H. S. Kim wrote the paper. J. Lee and H. S. Kim supervised the research. All authors analyzed data and discussed the results.